ENERGY HARVESTING DEVICE USING FERROFLUIDS SLUGS IN MICROCHANNELS

by

OMKAR AMAR PAWAR

Presented to the Faculty of the Graduate School of

The University of Texas at Arlington in Partial Fulfillment

of the Requirements

for the Degree of

MASTER OF SCIENCE IN MECHANICAL ENGINEERING

THE UNIVERSITY OF TEXAS AT ARLINGTON

DECEMBER 2018

ACKNOWLEDGEMENTS

I would like to dedicate this thesis to my late mother, it would have been impossible for me to complete the master program without her inspiration and blessings. I would like to thank my father for having faith in me. I would like to thank my sister who stood by me in every decision.

I express my gratitude towards my supervisor Dr. Hyejin Moon for providing me with the opportunity to perform research under her guidance. I still remember her words “Read. Act. Fail. Learn. Repeat” when I lost spirit due to repeated failure, which gave me the boost to keep on doing things till I overcome the problem. This made me an analytical thinker and helped me develop right perspective towards problem solving. I am thankful to her for providing the independence and making my master’s program a great learning experience.

Special thanks to my mentor Dr. Ali Farzbod for guiding me whenever I lost track of my research. I would also like to thank Dr. Mun Mun Nahar for helping me learn the COMSOL and being available to discuss the results of experiments and numerical study. I thank Dr. Arvind Venkatesan for helping me in numerous ways and for all the stress relieving talks we had. I thank to all my other lab-mates for their valuable inputs.

Finally, I would like to thank Vedha for having immense trust in my ability and always encouraging me to surpass my own limits. I would like to thank my friend Pranav Nikam for keeping a track of the progress of my research and for being one of the important factors for choosing The University of Texas at Arlington. I would like to thank my roommates, Sharon Chemmany, Pranav Jadhav, Swanand Jadhav and all my friends for their support and being a family away from my family.

ABSTRACT

ENERGY HARVESTING DEVICE USING FERROFLUIDS SLUGS IN MICRO-CHANNELS

Omkar Amar Pawar, MS

The University of Texas at Arlington, 2018.

Supervising Professor: Dr. Hyejin Moon

This research proposes a new concept of energy harvesting with the help of oscillating slugs of ferrofluid in microchannels. Ferrofluids are colloidal suspension of paramagnetic nanoparticles which get magnetized in the presence of magnetic field. They can conform to any shape and can be injected easily in intricate spaces. A change in the magnetic flux through the solenoid area produces electromotive force per Faraday's law. To prove the concept of harvesting energy by having a change in magnetic flux with the help of ferrofluids, several ferrofluid slugs were made to pass through a multi turn solenoid wound around a glass micro channel with the help of a fluid dispensing pump. Various parameters affecting the generation of the electromotive force are studied with the help of numerical study. A comparison between the experimental data and the results of finite element analysis using COMSOL Software has also been done. With progress in development of different energy harvesting device, using microfluidics for energy scavenging is still a novel concept which has a wide scope for advancement. The applications of the device proposed in this research include low wind energy harvesting.

TABLE OF CONTENTS

List of Illustrations

List of Tables

CHAPTER 1: INTRODUCTION

1.1 Motivation

Energy harvesting also known as energy scavenging is the process by which energy is derived from ambient external sources, captured, and stored for small, wireless autonomous devices, like those used in wearable electronics and wireless sensor networks [1].

The shrinking size of the electronic components reduce their power consumption, but it also makes the design intricate making it difficult to replace batteries from time-to-time. Researchers therefore propose of using an autonomous power generation device to supplement or completely replace the batteries. This would help reduce the cost of maintenance and prove as a viable option for sensors and actuators which are remotely located or are not easily accessible (e.g. inside nuclear reactors).

According to the U.S Energy Information Administration report published in 2018, about 80% of the energy needs are satisfied by non-renewable sources like fossil fuels. The rest 20% is contributed by nuclear power and renewable energy in percentage of 9% and 11% respectively. The faster rate of depletion of non-renewable fuels, adverse effect on environments motivates a desire of finding sustainable and clean source of energy to cater the global needs.

Thus, the need for sustainable source of energy and the desire to power sensor networks & mobile devices without batteries are the driving forces behind the search for new energy harvesting devices.

The history of energy harvesting date back to the windmill and the waterwheel. Researchers have come up with many innovative designs and methodologies to harvest energy. Mechanical vibration, temperature gradient, wind, solar, ocean energy, salinity gradient, etc. are converted by various forms of energy that an energy harvesting device taps into and generates potential difference.

Fig 1-1 Crystal Radio [2]

One of the earliest applications of ambient power collected from ambient electromagnetic radiation (EMR) is the crystal radio as shown in Fig 1-1. A crystal radio receiver, also called a crystal set, is a simple radio receiver, popular in the early days of radio. It uses only the power of the received radio signal to produce sound, needing no external power [2].

The basic principle of energy harvesting is converting the different types of ambient waste energy to either potential difference or current with the help of different physics phenomena. The following Fig 1-2 explains the general schematic of energy harvesting.

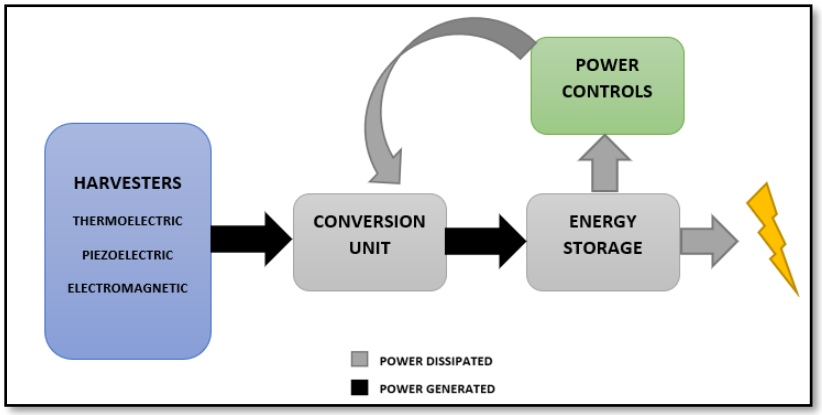

Fig 1-2 General Principle of Energy Harvesting [3]

1.2 Types of Electromagnetic Energy Harvesting

Energy harvesting device has become a focal area of research offering novel methods to provide continuous power supply to low power consuming electronics.

Among the various energy harvesting mechanisms, electromagnetic transduction has been investigated extensively in the open literature. Different configurations have been proposed, with the basic principle remaining the same; external excitement set a solid magnet in motion relative to a stationary coil.

Energy scavenging from different sources with the help of electromagnetism is briefly discussed in the following illustrations.

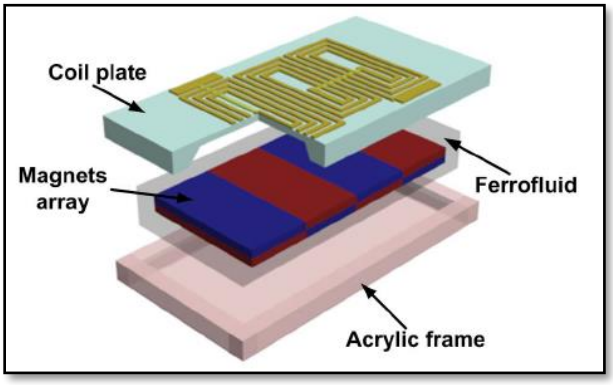

Fig 1-3 Geometry of vibration energy harvester [4]

Fig 1-3 shows an example of a vibration energy harvesting device [4]. In this device, the mechanical vibrations set the ferrofluid in motion. This disturbance in ferrofluid sets the suspended magnetic array in motion. Due to the movement of magnetic array in relation to the solenoids; there is a change of magnetic field perpendicular to cross section area of biplanar solenoid coils. This generates an electromotive force (EMF) based on the Faraday's law.

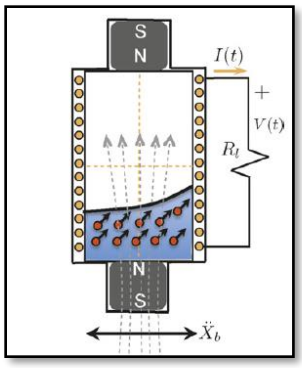

Fig 1-4 Working Principle of Sloshing Liquid Energy Harvester [5]

Fig 1-4 shows another example of electromagnetic energy harvester which uses mechanical vibration to produce change in magnetic field and thus generate EMF. In the above-mentioned device, a cylinder wound with solenoid coil is filled with ferrofluid. Two permanent magnets are placed at a certain distance to magnetize the ferrofluid but not make it rigid. The cylinder is excited due to mechanical vibrations which causes the ferrofluid to slosh, this leads to change in number of dipoles at the surface of ferrofluid. This causes a change in magnetization generating EMF [5].

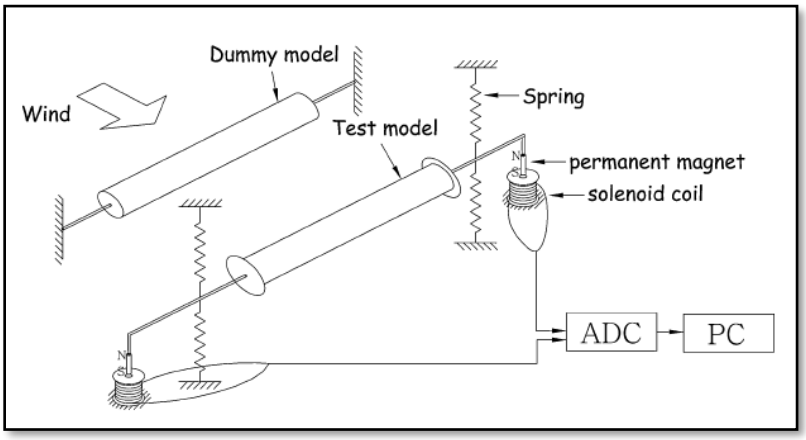

Fig 1-5 Schematic Representation of Energy Harvester [6]

The above shown example is harvesting the wind energy with the help of electromagnetism. Fig 1-5 shows the experimental setup of the energy harvesting device. In this setup, the laminar flow of wind when is obstructed by the buffer body or dummy model as shown in fig. This causes the laminar air flow

to become turbulent, which sets the test model cylinder to vibrate. The test model cylinder which is suspended with the help of spring oscillates up and down as a result of an aerodynamic instability known as wake galloping. These oscillations cause the permanent magnet attached to the end of cylinder to move in and out of the multi-turn solenoid coil. This relative motion of the magnets with respect to stationary coil leads to generation of EMF [6].

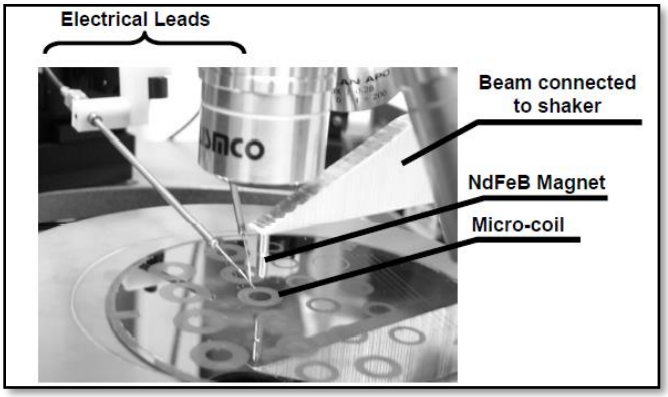

Fig 1-6 Set up of MEMS Fabricated Energy Harvesting Device [7]

Fig 1-6 shows another example of mems integrated electromagnetic energy harvester. In this example, there is relative motion between the two moving parts, a MEMS-based solenoid coil and NdFeB permanent magnet. The micro-solenoid is fabricated on the wafer [7]. The relative motion of the magnet due to external excitation with respect to the coil induces an EMF, or current, within the coil according to Faraday's law.

In this research, the use of ferrofluids as the magnetic material in electromagnetic energy harvesters is investigated.

1.3 Electromagnetic Induction

Electromagnetic induction is the phenomenon in which, an electromotive force (i.e., voltage) is generated across an electrical conductor when placed in a changing magnetic field. Voltage is generated in the conductor when it is moved through the magnetic field or when the magnetic field changes because, the magnetic lines of forces are applying a force on free electron in the conductor and causing them to move. The term induction is used for because there is no physical contact between conductor and magnet. One requirement for the electromagnetic induction to take place is that the conductor, must be perpendicular to the magnetic lines of force in order to produce the maximum force on the free electrons. The Faraday's law and Lenz's law are the two important laws which help to define the emf generated and the direction of current flow in any electromagnetic system considering some fundamental parameters [8].

1.3.1 Faraday's Law

Faraday's law of induction is a basic law of electromagnetism predicting how a magnetic field will interact with an electric circuit to produce an electromotive force (emf)—a phenomenon called electromagnetic induction. It is the fundamental operating principle of transformers, inductors, and many types of electrical motors, generators and solenoids [9].

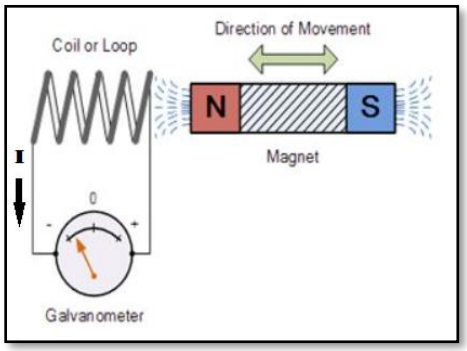

Fig 1-7 Faraday's Law

Fig 1-7 describes the principle of Faraday's law in which a moving bar magnet induces a current in the solenoid. Faraday's law of induction makes use of the magnetic flux ϕ through a region of space enclosed by a wire loop. The magnetic flux is defined by a surface integral:

$$\phi = \int_{\Sigma} B\,dA$$

where $d\mathrm{A}$ is an element of the surface Σ enclosed by the wire loop and B is the magnetic field. The dot product $B \cdot d\mathrm{A}$ corresponds to an infinitesimal amount of magnetic flux. In more visual terms, the magnetic flux through the wire loop is proportional to the number of magnetic flux lines that pass through the loop. When the flux through the surface changes, because B changes, or because the wire loop is moved or deformed Faraday's law of induction says that the wire loop acquires an electromotive force (emf).

So, the EMF generated by Faraday's Law can be given by rate of change of magnetic flux:

$$\varepsilon = -\frac{d\phi}{dt}$$

Where, $\mathcal{E}$ is the Electromotive Force (EMF) and ϕ is the Magnetic Flux. For a loop with N number of turns, the formula is:

$$\varepsilon = -N\frac{d\phi}{dt}$$

Using the definition of magnetic flux, the above-mentioned equation can be further simplified to:

$$\varepsilon = -N\int \frac{dB}{dt}\,dA$$

So, it is learned that the emf generated depends upon how fast the magnetic field change, the magnitude of change in magnetic field and the cross-sectional area of coil [11].

1.3.2 Lenz's Law

The Faraday's law gives the magnitude of the induced emf, but it is the Lenz's law that gives the direction of the induced emf.

The Lenz's law states that when an emf is generated by a change in magnetic flux according to Faraday's law, the polarity of the induced emf is such that it produces a current whose magnetic field opposes the change which produces it. The induced magnetic field inside any loop of wire always acts to keep the magnetic flux in the loop constant [12].

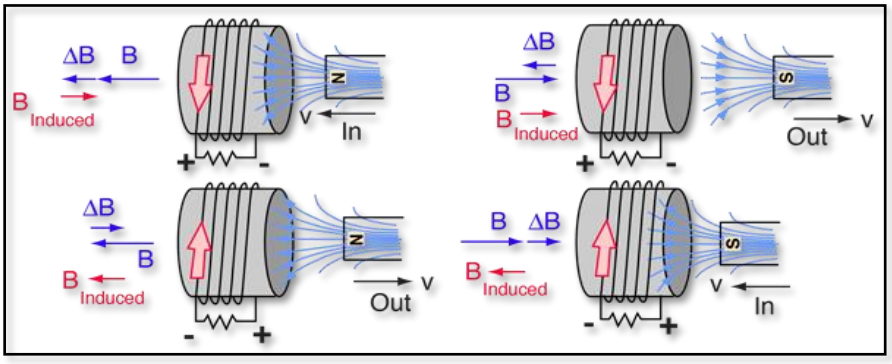

Fig 1-8 Lenz's law [13]

In the Fig 1-8 shown above, if the B field is increasing, the induced field acts in the direction opposite to it. If it is decreasing, the induced field acts in the direction of the applied magnetic field to try to keep magnetic energy in solenoid constant.

1.4 Ferrofluids

Ferrofluids are colloidal liquids made of nanoscale paramagnetic Fe_3O_4 particles suspended in a carrier fluid. The Ferrofluids are colloidal suspensions – materials with properties of more than one state of matter. In this case, the two states of matter are the solid metal and liquid it is in. This ability to change phases with the application of a magnetic field allows them to be used as seals, lubricants, and may open up further applications in future nanoelectromechanical systems. A grinding process for

ferrofluid was invented in 1963 by NASA's Steve Papell as a liquid rocket fuel that could be drawn toward a pump inlet in a weightless environment by applying a magnetic field [14].

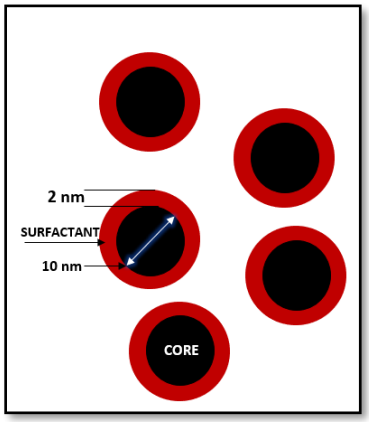

Fig 1-9 Schematic Representation of Fe_3O_4 Nanoparticles in Ferrofluid

The nanoparticles are coated with adsorbed surfactant layers to prevent particle agglomeration due to the Van der Waal's force and dipole-dipole interactions among them. Fig 1-9 shows the schematic representation of ferrofluid nanoparticle adsorbed with surfactant. The particles in a ferrofluid primarily consist of nanoparticles which are suspended by Brownian motion and truly stable. This means that the solid particles do not agglomerate, or phase separate even in extremely strong magnetic fields. However, the surfactant tends to break down over time of few years, and eventually the nanoparticles will agglomerate, and they will separate out and no longer contribute to the fluid's magnetic response. Ferrofluids usually do not retain magnetization in the absence of an externally applied field and thus are often classified as "superparamagnets" rather than ferromagnets.

A regular pattern of peaks and valleys is formed when ferrofluids are subjected to strong magnetic field perpendicular to its area of spreading as shown in Fig 1-10. This effect is known as the Rosensweig or normal-field instability. The instability is driven by the magnetic field; it can be explained by considering which shape of the fluid minimizes the total energy of the system [14].

Fig 1-10 Ferrofluid Peaks and Ridges

From the point of view of magnetic energy, peaks and valleys are energetically favorable. In the corrugated configuration, the magnetic field is concentrated in the peaks; since the fluid is more easily magnetized than the air, this lowers the magnetic energy. In consequence the spikes of fluid ride the field lines out into space until there is a balance of the forces involved.

At the same time the formation of peaks and valleys is resisted by gravity and surface tension. It requires energy for both to move fluid out of the valleys and up into the spikes, and to increase the surface area of the fluid. To summarize, the formation of the corrugations increases the surface free energy and the gravitational energy of the liquid, but reduces the magnetic energy. The corrugations will only form above a critical magnetic field strength, when the reduction in magnetic energy outweighs the increase in surface and gravitation energy terms.

Depending upon the type of suspension liquid, the ferrofluids are classified in two categories:

- Water Based Ferrofluid- This range of ferrofluids use deionized water as the suspension liquid. E.g. Ferrotec Inc. ferrofluid series EMG 700, EMG 305, EMG 705, etc. [15]
- Oil Based Ferrofluid- This range of ferrofluids use hydrotreated light petroleum distillates as the suspension liquid. E.g. Ferrotec Inc. ferrofluid series EMG 900, EMG 901, EMG 905, EMG 909, EMG 911, etc. [16]

The following table describes in detail the various physical, chemical and magnetic properties of the different ferrofluid considered for the research:

Table 1-1 Different ferrofluids and their Properties [17]

PROPERTY	EMG 700	EFH 1	EMG 901
Carrier Fluid	Light Hydrocarbon Oil	Water	Light Hydrocarbon Oil
Density	1350 kg/m^3	1290 kg/m^3	1430 kg/m^3
Magnetization	440 Gauss	325 Gauss	660 Gauss
Viscosity	6 cP	5 cP	8 cP
Magnetic Particle Concentration	9% by volume	5.8% by volume	11.8% by volume

CHAPTER 2: NUMERICAL SETUP

2.1 Introduction

To get better understanding of the changes occurring in the experiment device, COMSOL Multiphysics, a finite element analysis (FEA) solver and simulation commercial software was used for this study. Finite element analysis is a numerical approach for calculating solution of a problem by applying required boundary conditions and initial values. The numerical methods help to give approximate values of the unknown parameters at discrete number of points in the continuum. In the finite element method, rather than solving the problem for the entire body in one operation, we develop the equations for each finite element and combine them to get the solution of the entire system. We also used COMSOL Multiphysics to perform parametric study. We used fluid flow and AC-DC Module for simulations. [18] [19]

2.2 Fluid Flow Module

2.2.1 Modeling

A 3-Dimensional two-phase model was built using the COMSOL Multiphysics software. Making the dimensions as close to the experimental set-up and selecting the right physics was the first step of this study. A 3-D CAD model was built to resemble the experimental setup.

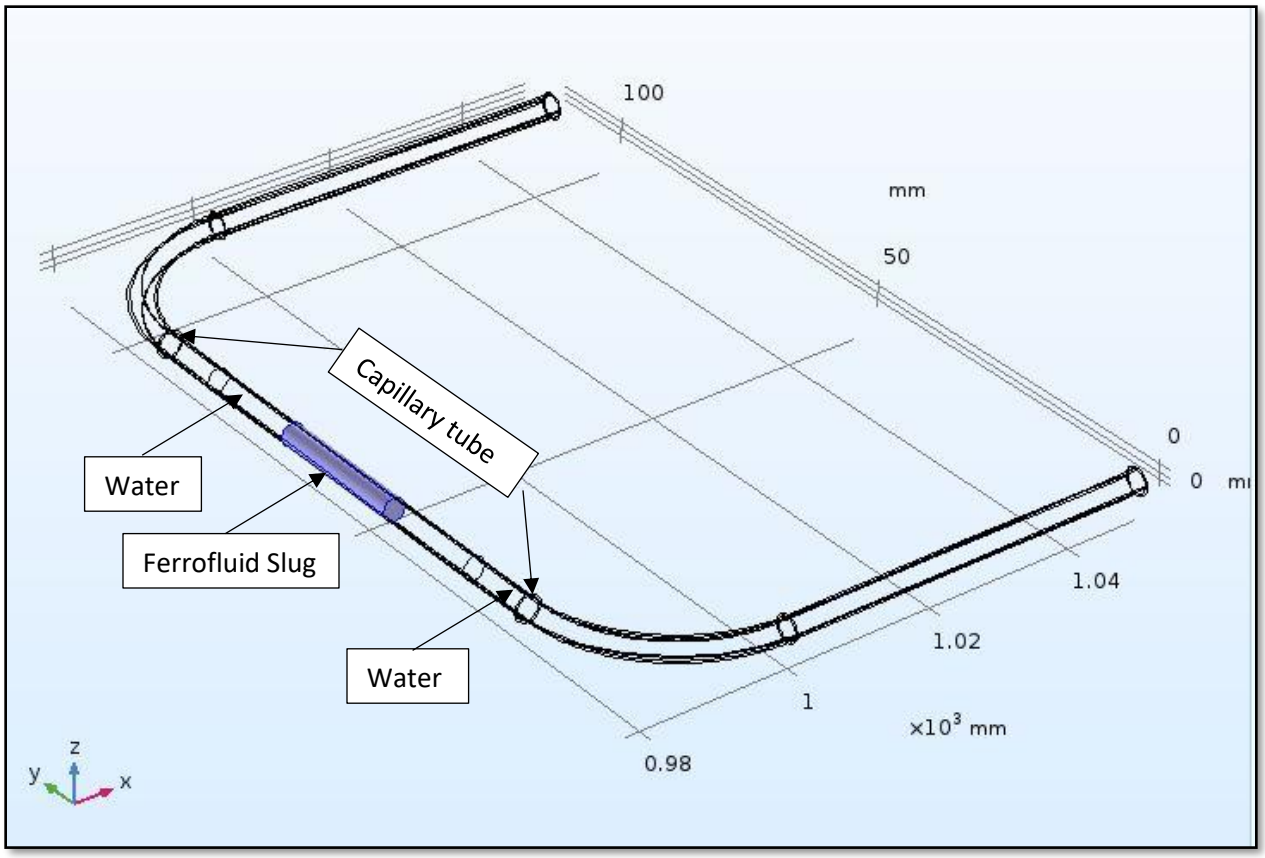

Fig 2-1 Geometry of Fluid Flow Model

As seen in Fig 2-1, an EFH 1 ferrofluid slug is considered in water environment. The dimensions of the CAD model are given in detail in table below.

Table 2-1 Dimensions of CAD Model

Part Name	Diameter(mm)	Length(mm)
EFH-1 Slug	1.5	20
Capillary Tube	1.5	70
Tubing	1.5	-

For the slug, properties of ferrofluid EFH-1 are assigned and the rest of the medium is water.

2.2.2 Governing Equations

Oscillation of slug concerns with only one physics; fluid dynamics, hence this physics is chosen for study. In fluid flow, two phase laminar flow is considered, and level set equations are chosen for interface tracking. In the previous step, geometry is built up and material properties are assigned to it and in this step, fluid flow physics are being setup. For fluid flow, an incompressible, time dependent Navier-Stokes equation is used.

$$\rho\, \partial u/\partial t + \rho(u.\nabla) = \nabla.[-pI + \mu(\nabla u)^{T})] + F$$

$$\rho\nabla.(u) = 0$$

2.2.3 Initial Condition

Velocity is considered zero and atmospheric pressure and temperature were considered.

2.2.4 Boundary Conditions

For fluid flow domain, no slip boundary condition was provided for the slug-wall boundary as shown in Fig 2-2.

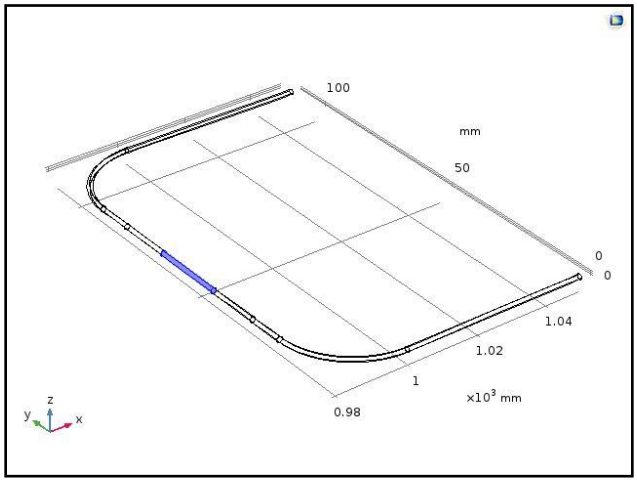

Fig 2-2 No Slip Boundary Condition Domain

The no slip condition is given by the equation, $K - (K \cdot n)n = 0$; where $K = [\mu(\nabla u + (\nabla u)^T]n$. The initial interfaces were selected as shown in Fig 2-3.

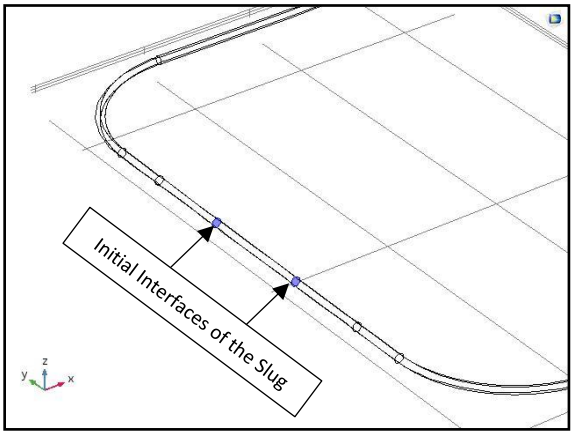

Fig 2-3 Initial Interfaces

For the Level Set equations for interface tracking, wetted wall condition was selected between the slug and the walls. The wall was assumed to be hydrophobic and thus, the contact angle (θ_ω) selected was 120^o.

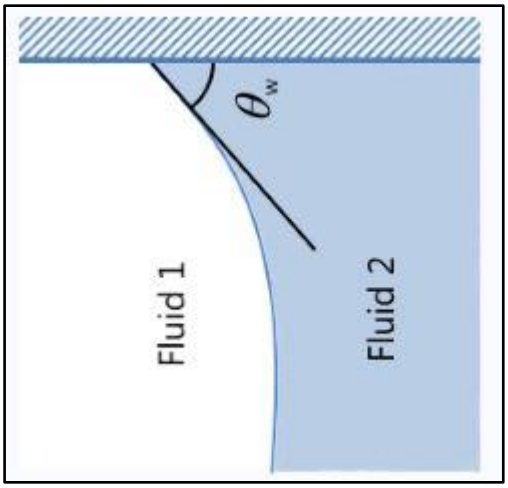

Fig 2-4 Contact Angle of the two fluids with glass capillary tube

Boundary stress was applied to both the openings of the tube because, since the flow is always oscillating, an opening cannot be constrained to be an inlet or an outlet.

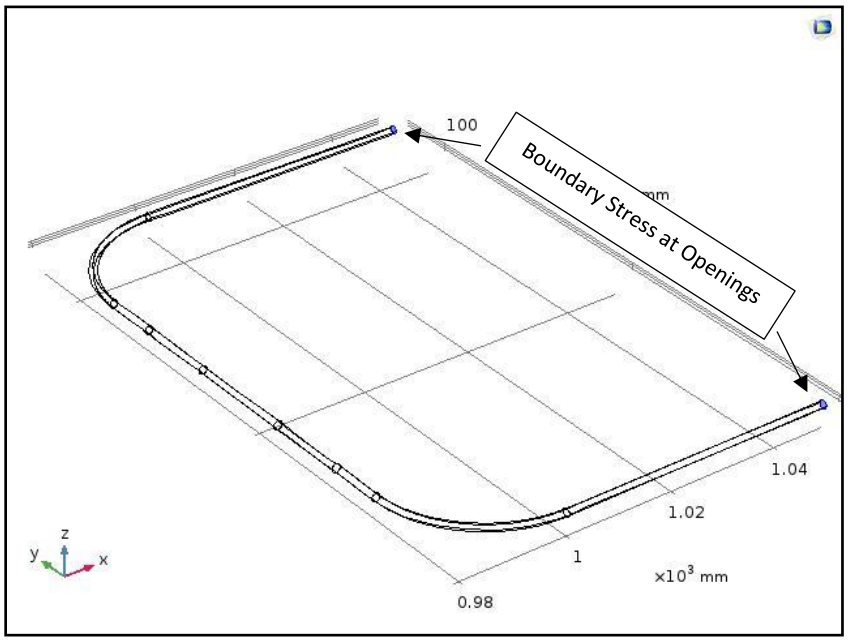

Fig 2-5 Boundary stress at openings of the tube

2.2.5 Meshing

Meshing is the process of dividing the geometry in numerous finely divided elements. User-defined meshing was used in this model which gives liberty to finely mesh only the areas of the interest. The tetrahedral mesh elements were used in this case. Fig 2-6 shows the completely meshed model.

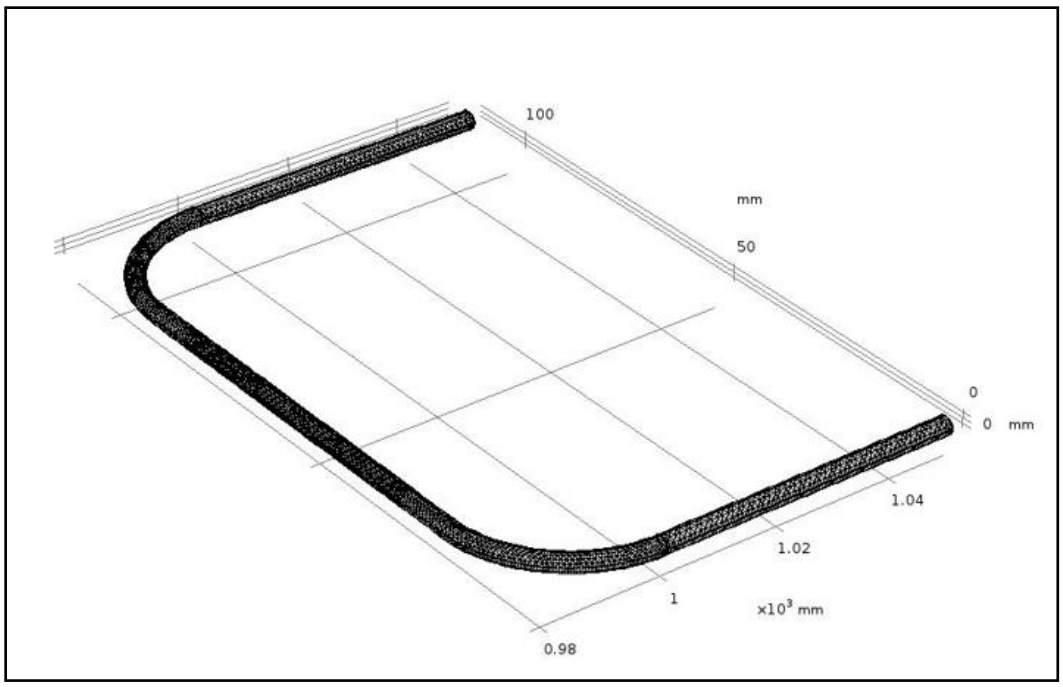

Fig 2-6 Meshed Model

2.2.6 Solution

After meshing, with the help of an integrated COMSOL MULTIPHYSICS solver we compute the solution. Since this is time dependent study hence, we must define the time (name of solver).

2.2.7 Result

Once the solution is computed, the oscillating slug motion was achieved. The velocity of the moving slug is determined from the simulation. The oscillating slug video link:

https://drive.google.com/open?id=1Wy-LPm_xuZz9vmKwg6RuWiJSI-N8GhVJ

2.3 ELECTROMAGNETIC MODULE

2.3.1 Modeling

A 2-Dimensional model was built using the COMSOL Multiphysics software. Making the dimensions as close to the experimental set-up and selecting the right physics was the first step of this study. A 3-D CAD model was built by revolving about an axis to resemble the experimental setup.

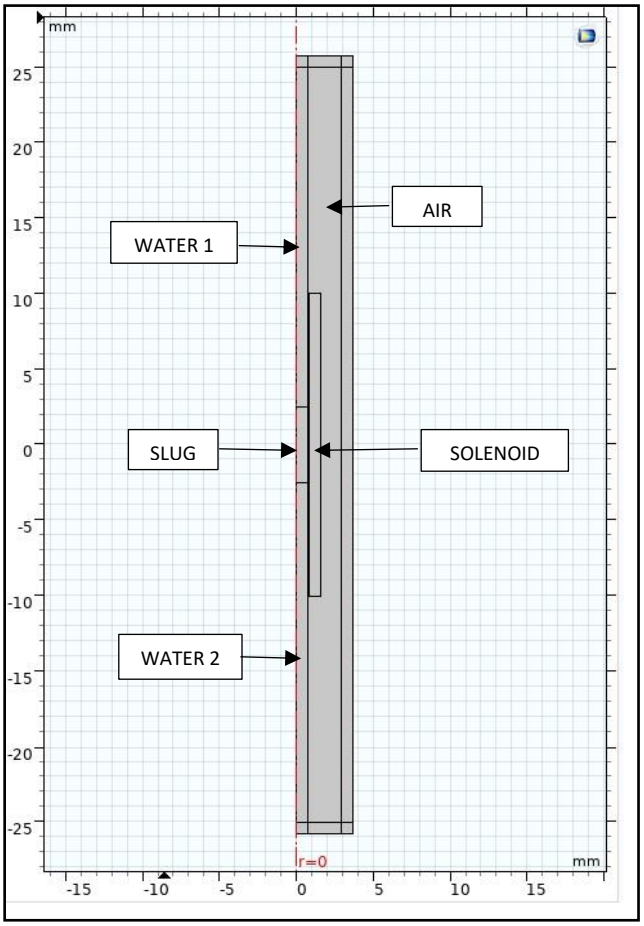

Fig 2-7 Geometry of Electromagnetic Model

As seen in Fig, the EFH1 slug is considered in water environment. A 40 AWG copper coil solenoid is assumed around the capillary tube. The dimensions of the CAD model are given as follows:

Table 2-2 Dimensions of CAD Electromagnetic Model

PART NAME	LENGTH (mm)	BREADTH (mm)
SLUG	5	0.75
WATER	25	0.75
COIL	20	0.27
AIR	50	3

2.3.2 Governing Equations

Moving mesh method is used to resemble the motion of the oscillating slug in the electromagnetic model. The predefined deformations of domains for the moving mesh are given by the simple harmonic equations. Since the slug oscillates between two defined extreme points, we define the deformation of the domains based on these harmonic equations as follows:

For slug, $15\sin(2\pi f_0 t)$

For water 1, $15\sin(2\pi f_0 t)(\frac{(25-Z)}{22.5})$

For water 2, $15\sin(2\pi f_0 t)(\frac{(25+Z)}{22.5})$

To calculate the voltage induced, different properties of the materials are considered to build the equations.

The governing equations for the physics of electromagnetic induction are the ampere's law:

$$\nabla \times H = J$$

$$B = \nabla \times A$$

$$J = \sigma \times E$$

where, *B* is the magnetic flux density, *H* is magnetic field strength, *J* is current density, *A* is the area through which magnetic flux lines pass and *E* is the electric field.

The magnetic field is described distinctively for the Ferrofluid and the rest of the domains. To calculate the magnetic flux density for the ferrofluid, the Saturation Magnetization (*M*) is considered along with the magnetic field strength (*H*) contributed by the solenoid when the voltage is induced. Saturation Magnetization (*M*) is the maximum magnetization in reached by the magnetic materials when in an external magnetic field.

Table 2-3 Saturation Magnetization Values of Different Ferrofluids

FERROFLUID	SATURATION MAGNETIZATION (GAUSS)
EFH 1	440
EMG 700	325
EMG 901	660

The Fig 2-8 shows the highlighted ferrofluid slug and the equation for determining the magnetic flux density is $B = \mu_0(H + M)$

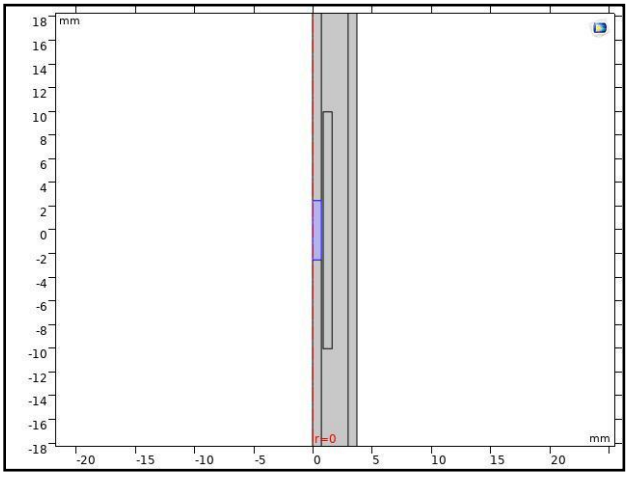

Fig 2-8 Domain for Ampere's Law based on Saturation Magnetization

The magnetic permeability (μ_o) and the relative permeability (μ_r) of the water/air are considered for calculating the effect of change in magnetic flux in the surrounding medium due to oscillating slug. The Fig 2-9 shows the highlighted domain for which these parameters are considered.

The magnetic flux density is given by $B = \mu_o \mu_r H$

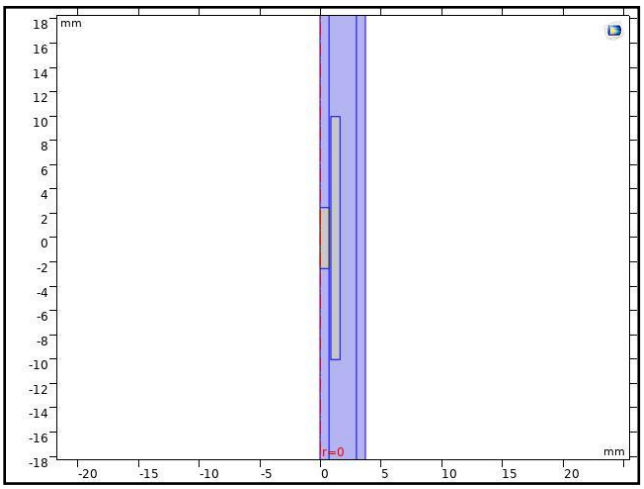

Fig 2-9 Domain for Ampere's Law based on Relative Permeability

2.3.2.1 Coupling Slug Velocity to Frequency

The electromagnetic model requires frequency (f_0) as an input parameter. The velocity of the slug obtained from the Fluid Flow model was converted to frequency with the help of following relation.

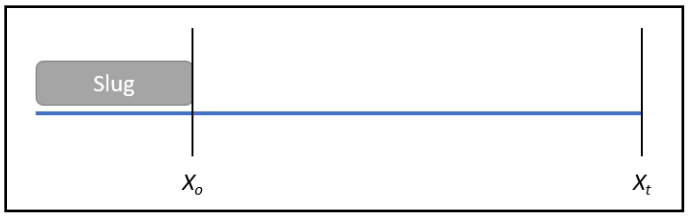

Fig 2-10 Coupling Slug Velocity to Frequency

$$f_0 = \frac{velocity\ of\ slug}{X_t - X_0}$$

2.3.3 Boundary Conditions

There are two types of boundary considered in the Electromagnetic Model. The Magnet Boundary and the Infinite Boundary. The magnet boundary was applied to all the boundaries of ferrofluid slug domain as shown in Fig 2-11.

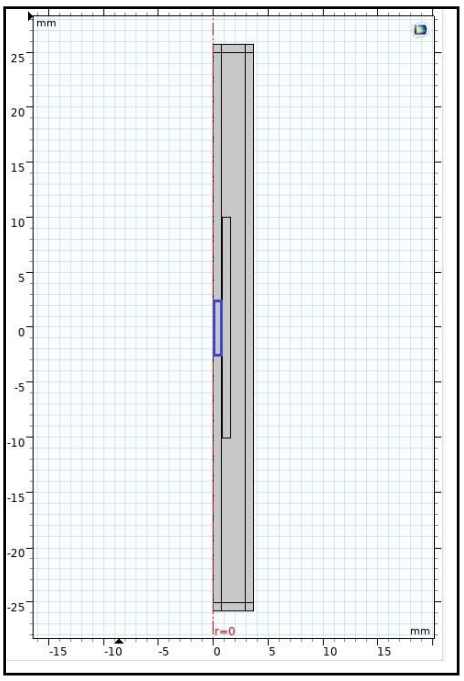

Fig 2-11 Magnetic Boundaries

The infinite boundary is applied to edges of the air domain. This boundary condition makes the air domain a continuous large space as it would be in practical experiments. The infinite boundaries are highlighted in the Fig 2-12.

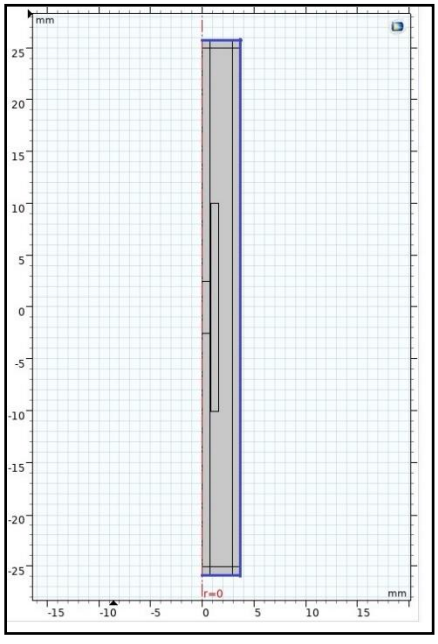

Fig 2-12 Infinite Boundaries

2.3.4 Solution

In order to solve for the voltage, you must take the integral of the magnetic fields over domains of the flashlight. The AC/DC Module of COMSOL Multiphysics contains a series of interfaces and functionality that allow to do so based on the domain boundaries involved, among other factors.

This was a two-step process. First, we performed a stationary analysis of the magnetic fields. Doing so allowed us to provide the appropriate initial conditions for performing the second step: a transient analysis of the magnetic fields.

2.3.5 Result

Once the solution is computed, the oscillating slug motion was achieved. The voltage induced in the coil was obtained in the form of voltage-time plot. Various coil voltage induced plots have been discussed in the next chapter.

CHAPTER 3: PARAMETRIC STUDY

3.1 Introduction

Parametric studies allow you to nominate parameters for evaluation, define the parameter range, specify the design constraints, and analyze the results of each parameter variation. This study was performed to see the effect of change of different dimensions, working conditions as well as the physical properties. The parameters that were considered for this study were pressure, diameter, magnetization and slug-to-coil ratio.

3.2 Pressure

For this study, three different pressures were selected viz; 1.25 bar, 1.5 bar and 2 bar. The diameter of the capillary tube was kept constant at 1.5mm, the no. of turns of coil were at 900 and the ferrofluid selected was EFH1. The length of the slug was 20mm and smaller than the length of the coil. The higher the pressure the higher is the slug velocity as seen in Table 3-1.

Table 3-1 Velocity of Slug at Different Pressure

PRESSURE (bar)	VELOCITY(m/s)
1.25	1.89
1.50	2.41
2.00	3.00

The voltages induced in the coil were 4.5 mV, 5.5 mV and 6.5 mV for 1.25 bar, 1.5 bar and 2 bar respectively can be seen in Fig 3-1. The peaks of the voltage generated occurred at same frequency for all three pressures due to same slug length to coil length ratio.

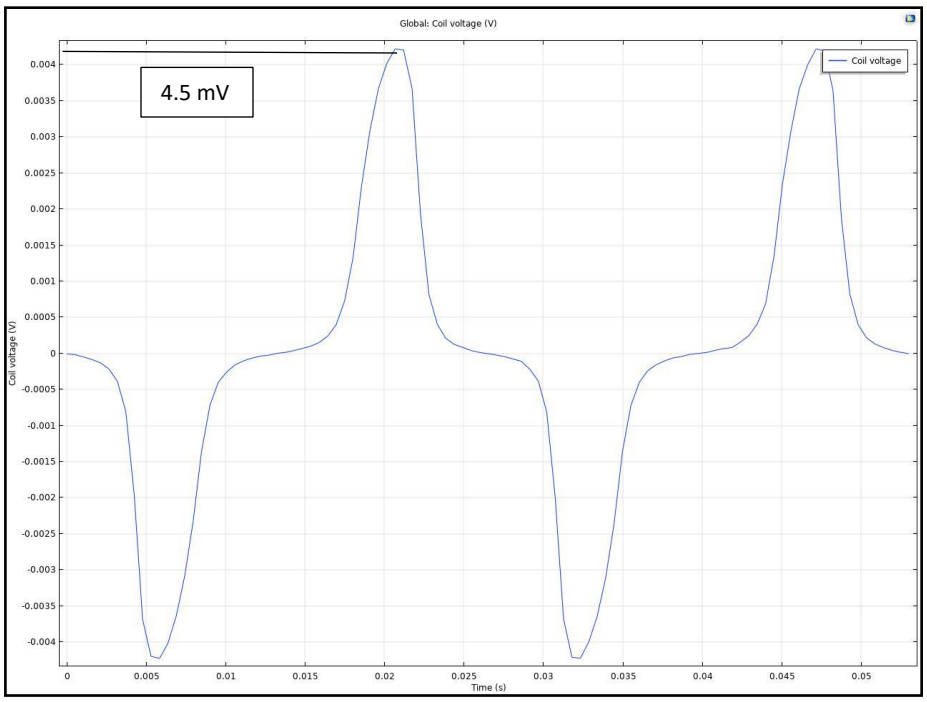

Fig 3-1 Induced Coil Voltage Graph At 1.25 Bar Pressure

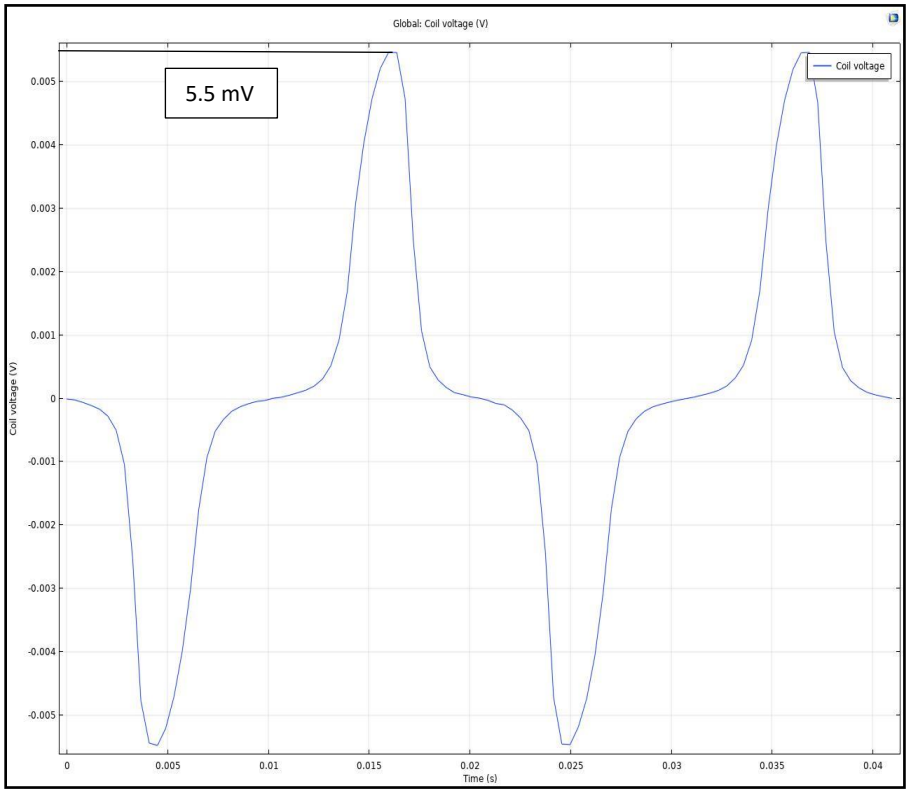

Fig 3-2 Induced Coil Voltage At 1.5 Bar Pressure

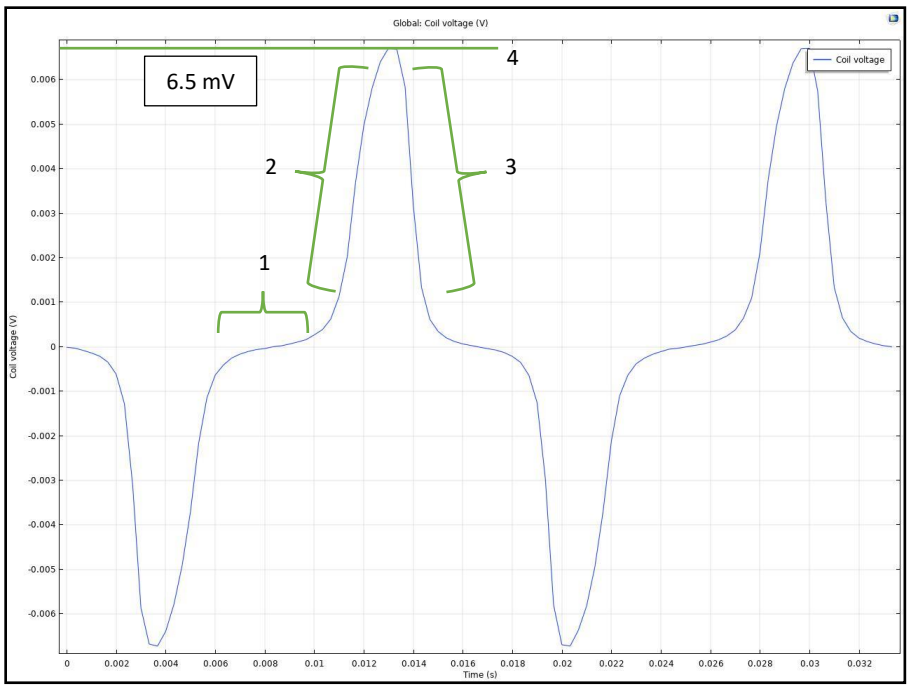

Fig 3-3 Induced Coil Voltage At 2 Bar Pressure

No voltage is generated when the slug is completely outside the solenoid as seen in region 1. The rising slope (region 2) to the peak indicates that the slug is entering the solenoid. When the slug is completely inside the solenoid the voltage peak is attained as a result of maximum change in magnetic field (region 4). The voltage induced starts to descend during the exit of slug from the solenoid as indicated by region 3. The induced voltage shows reverse polarity when the slug enters the solenoid again from the opposite direction per Lenz's law. The higher velocity corresponds to higher frequency and hence higher voltage as seen in Fig 3-2.

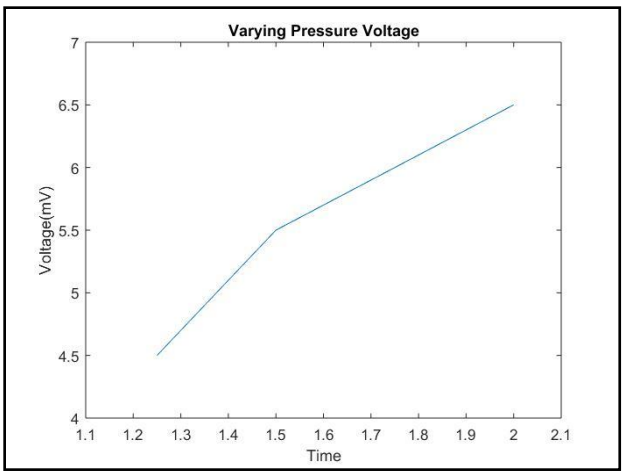

Fig 3-4 Comparison of Peak Voltages at Different Pressure

3.3 Diameter

For this study, different diameters of capillary tube were considered for simulation. The different diameters were 150um, 1.5mm, 2mm, 2.5mm, 3mm, 4mm, 5mm. The pressure was kept constant for all the diameters at 2 bar, the no. of turns of coil were at 900 and the ferrofluid slug properties were those of EFH1. The length of the slug was 20mm and smaller than the length of the coil. An interesting observation was noted. The increase in diameter corresponded to increase in velocity but this held true only up to certain diameter. The slug formation phenomenon is governed by the surface tension. As the diameter increases the surface tension starts getting weaker and the gravity effect takes its place. This results in decrease in slug velocity because of viscous drag and failure to form the slug. Thus, to successfully have slugs for energy harvesting we must have capillary number smaller where the surface tension is stronger and gravity can be neglected. The Fig 3-3 shows the graph of diameter vs velocity.

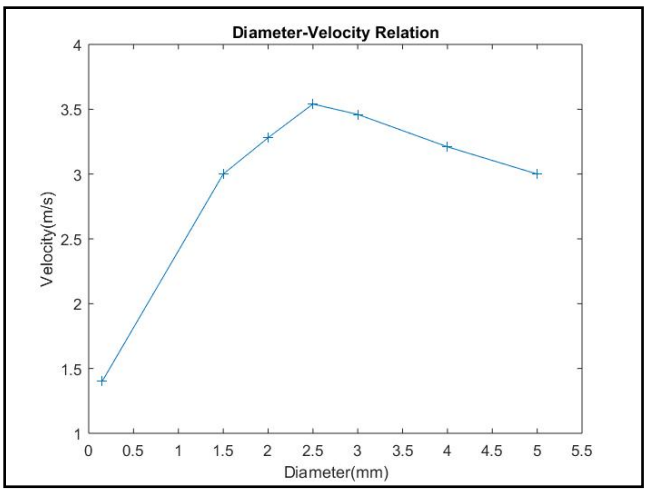

Fig 3-5 Comparison of Slug Velocities at Different Diameters

According Faraday's law, the emf generated is directly proportional to the no. of turns of coil, change in magnetic flux, area through the magnetic flux lines cut and frequency. However, the decrease in velocity does not affect the generation of voltage even if it corelates to drop in frequency since both change in magnetic flux and area through which magnetic flux lines cut increase with increase in diameter. A greater change in magnetic flux is achieved by increase in diameter because as the diameter increases, higher volume of ferrofluid passes through the solenoid. Higher volume of ferrofluid corresponds to greater change in magnetic field. The voltage induced in the coil were 6.5 mV, 12 mV, 20 mV, 28 mV, 42 mV, 57 mV for diameter of 1.5 mm, 2 mm, 2.5 mm, 3 mm, 4 mm, 5 mm respectively. The Fig 3-4 shows the diameter vs voltage graph.

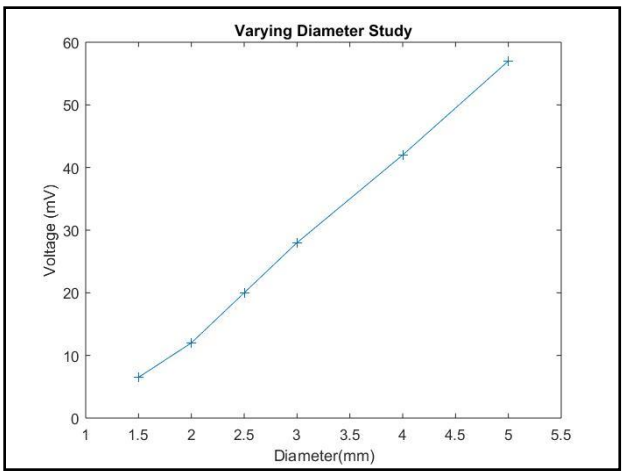

Fig 3-6 Comparison of Peak Voltages for Tubes with Different Internal Diameter

3.4 Magnetization

The magnetization of ferrofluids depends on their value of saturation magnetization. The three different ferrofluids selected for this study were EFH 1, EMG 700, EMG 901 and their saturation magnetization was 440 Gauss, 325 Gauss and 660 Gauss respectively. The pressure was kept constant at 2 bar, capillary diameter was kept constant at 1.5mm and no. of turns of coils were fixed at 900. The length of the slug was 20mm and smaller than the length of the coil. The change in magnetization brought by the ferrofluid slug is directly proportional to the saturation magnetization of ferrofluid used. The Fig 3-5 shows the magnetization vs voltage graph for all the ferrofluids.

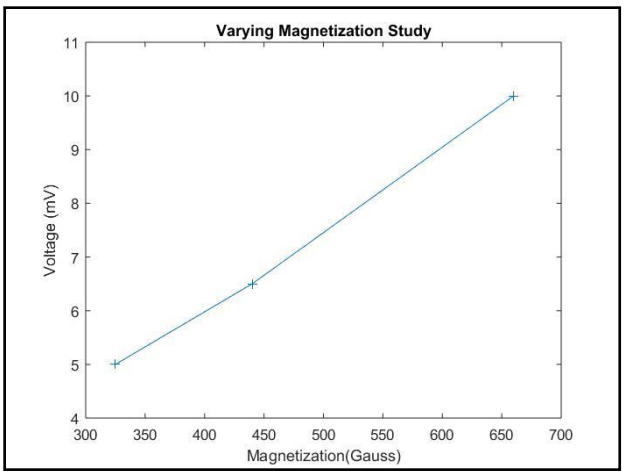

Fig 3-7 Comparison of Peak Voltages for Different Magnetization of Different Ferrofluids

3.5 Slug to Coil Ratio

Another aspect which was studied and has significant importance on the voltage induced is the ratio of slug length to coil length. When the slug length (20 mm) is equal to the coil (20 mm), the voltage induced is 8 mV with almost continuous peaks as shown in Fig 3-6. The voltage induced in the coil when the slug length (20mm) is longer than coil length (5mm) is higher about 30 mV, but the frequency of voltage peak generation is reduced as shown in Fig 3-7. If we integrate the voltage generated over a period then it is understandable that we will find the voltage generated by slug with length equal to coil higher than that of the slug with length longer than coil length. So, the optimum length for the slug where the amplitude as well as the frequency of voltage generation is maximum will be the instances where slug length is equal to coil length.

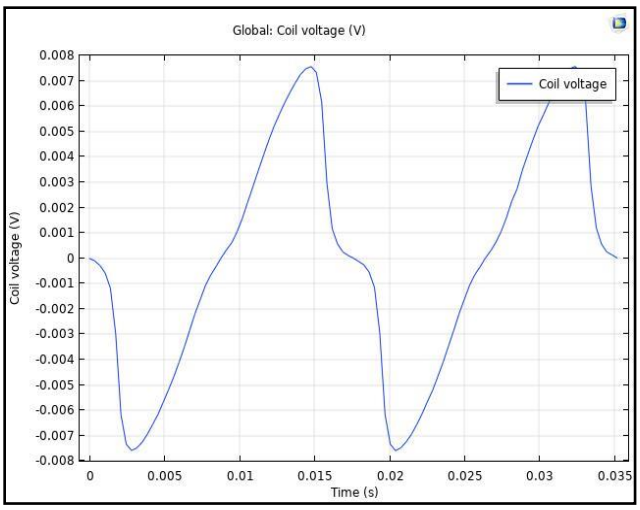

Titles for Axes

X-axis – Coil Voltage [V]

Y-axis – Time [secs]

Fig 3-8 Coil Voltage Induced when Slug Length is equal to Coil Length

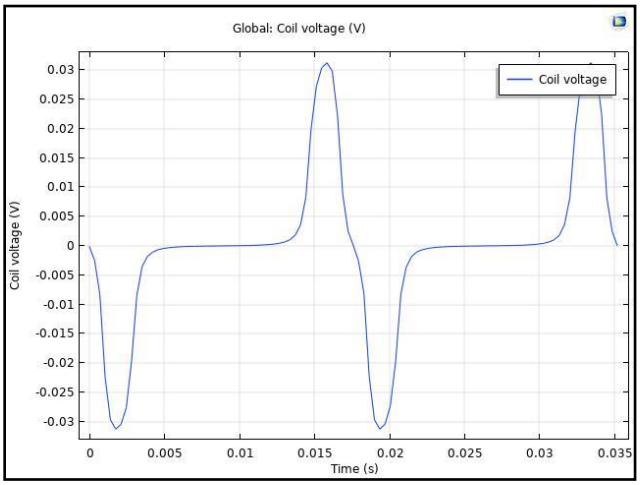

Titles for Axes

X-axis – Coil Voltage [V]

Y-axis – Time [secs]

Fig 3-9 Coil Voltage Induced when Slug Length is Longer than Coil Length

CHAPTER 4: EXPERIMENTAL SETUP

4.1 Overview and Experimental Setup

In order to verify the concept of induced emf by oscillating a slug in capillary tube, an experimental set up was designed and fabricated. In this experiment, EFH 1 was used as ferrofluid. EFH 1 is an oil based ferrofluid. An EFH 1 slug is created in the water environment.

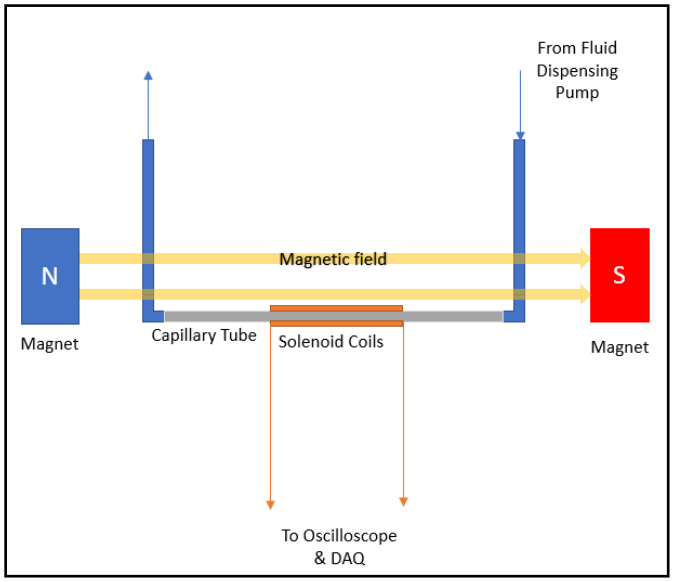

Fig 4-1 Schematic Representation of Design of Device

Unlike the simulation set up, ferrofluid slug is not made to oscillate in & out of solenoid but a train of ferrofluid slugs is made to pass through the solenoid coil since achieving the oscillation of ferrofluid slug is difficult.

Fig 4-1 shows the schematic representation of the device. The glass capillary tube with 1.5 mm internal diameter is used with a length of 50 mm. Additional plastic tubes with inner diameter 1.5 mm are connected to the capillary tube to help connect the capillary tube to the fluid dispensing pump. N 45 grade permanent Neodymium magnets are used to magnetize the ferrofluid. The solenoid was made by winding 40 AWG insulated Copper Wire in 900 no. of turns on the capillary tube. The device set up is as shown in the Fig 4-2.

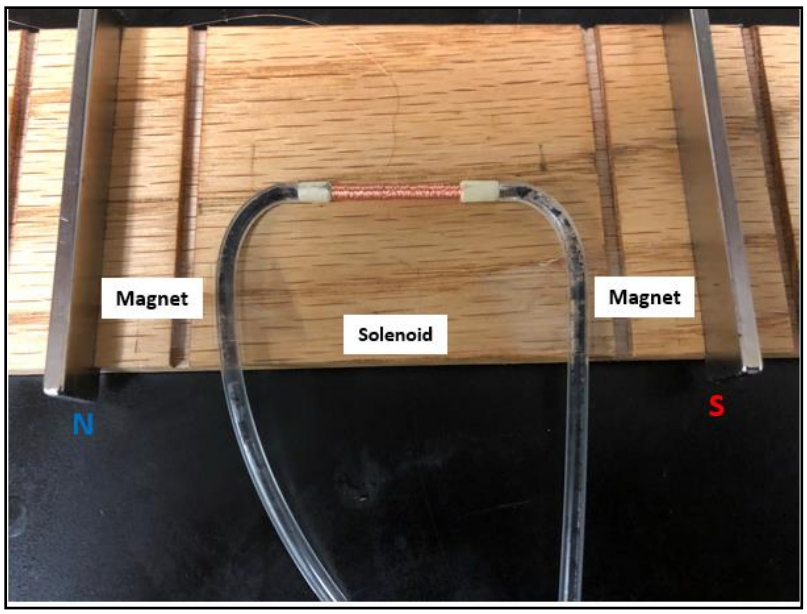

Fig 4-2 Experimental Setup of Energy Harvesting Device

The experimental set up is as shown in the Fig 4-3. Performus VII fluid dispensing pump is used for applying desired pressure to the slugs in both capillary and plastic tubes. The simulation results showed the output voltage to be in range of mV. Thus, to amplify the output voltage, the solenoid leads are connected to a non-inverting Op-Amp 741 amplification circuit. The amplifier circuit is powered by a 14 V DC power supply by hp 6038A. The output from the amplifier is then fed to Tektronix 2232 oscilloscope and Keithley 2700 DAQ.

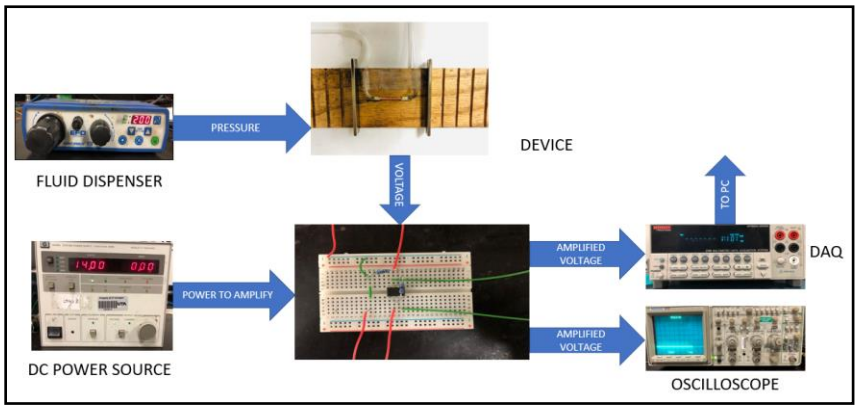

Fig 4-3 Experimental Setup

4.2 Experiment Procedure

The ferrofluid was injected in the plastic tubes with the help of syringes alternately with water. The flexible plastic tube is then connected to the paddle operated Performus VII fluid dispensing pump. To match the velocity of the slug from simulation, pressures of same magnitudes were applied to slug. The pressure is precisely set at 1.25 bar, 1.5 bar and 2 bar for each run of experiment. The DC power supply is switched on and set at 14 V and connected to the amplifier. The oscilloscope is switched on and the output wires from the amplifier are connected to Channel 2. The oscilloscope is adjusted for 20 mV/division scale for the Y-axis and 1ms/division for X-axis. The Keithley 2700 is then connected to the PC which serves the purpose of DAQ with the help of LabView programming.

As soon as the paddle was pressed, the ferrofluid slug moved through the tubes and through the solenoid coil. The ferrofluid got magnetized as it entered the magnetic field of permanent magnets. The spikes in the voltage graph were seen, which showed that the voltage has been generated.

CHAPTER 5: RESULTS AND ANALYSIS

Upon stepping on the paddle, the magnetized ferrofluid slug moves through the solenoid. The ferrofluid slug causes a change in magnetic flux through the solenoid area. This results to induction of voltage per Faraday's Law.

Higher the pressure, the slug moves with higher velocity which induces greater voltage in the coil. The same pattern was observed from the experiment data. However, the experimental result varies from the simulation result for some defined reasons.

The Fig 5-1 shows the experimental value of the induced voltage for the pressure of 1.25 bar, 1.5 bar and 2 bar.

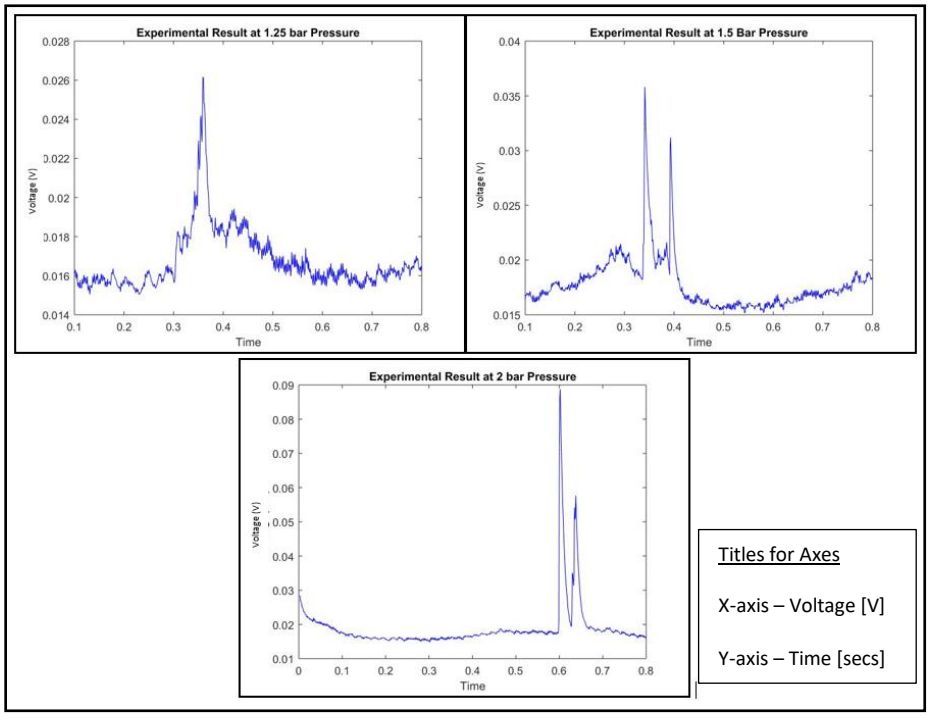

Fig 5-1 Experimental Output of the Voltage Induced at different Pressures

The spike observed in the graph indicates the induced voltage. The pattern of the spike in the graph is self-explanatory. As the slug moves in the solenoid, a change in total magnetic energy in the

solenoid area occurs which induces emf. As the slug moves furthermore in the solenoid coil the voltage induced steeply rises.

The voltage peak attains the maximum value when the slug is completely inside the solenoid coil because the maximum change in magnetic field is experienced by the solenoid coil. The voltage peak value drops as the slug moves further ahead because decrease in magnetic energy occurs and the value of induced voltage drops to noise value when the slug exits the solenoid completely.

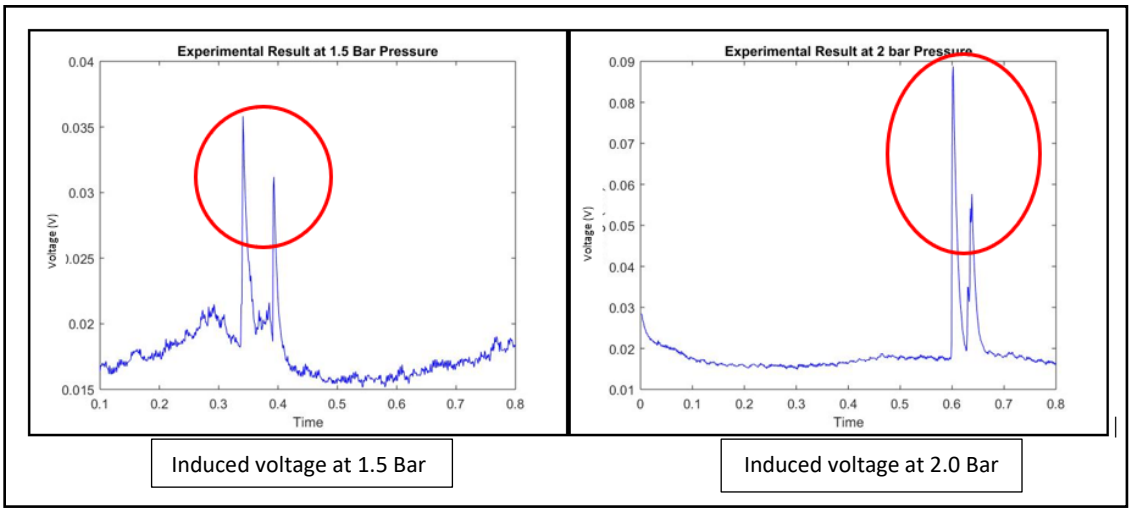

Fig 5-2 Effect of the Distortion of the Slug on Voltage Induced

The two peaks in the Voltage VS Time graph of 1.5 bar and 2 bar pressure as shown in Fig 5-2 indicates the distortion of the slug. The reason for slug distortion being the different viscosities of the two liquids. Since the viscosity of the water (1 cP) is less than that of the ferrofluid (6 cP) used in experiments, the velocity with which both the liquids move at same pressure applied is different. Due to lower viscosity the water travels at a higher velocity than the ferrofluid, which results into water breaking the slugs.

The magnitude of the induced voltage in the experimental study is lower than that of the simulation result. The reason for values of the voltage induced in the coil to vary from that of the simulation results is velocity and distortion of slug. Even though we matched the pressure condition at the inlet of the tube, the velocity of the slug was still slower than that simulated by COMSOL. Table 5-1 shows the comparison in the simulation and experimental result.

Table 5-1 Comparison of Voltages Induced

PRESSURE (bar)	SIMULATION RESULT (mV)	EXPERIMENT RESULT w/ NOISE (mV)	EXPERIMENT RESULT w/o NOISE (mV)
1.25	4.5	0.26	0.10
1.50	5.5	0.35	0.15
2.00	6.5	0.9	0.7

CHAPTER 6: CONCLUSION

A numerical & experimental study has been performed on the proposed principle of energy harvesting. The conclusions drawn from the study are as follows:

1) The Energy Harvesting Device generates 0.7 mV at 2 bar pressure, 0.15 mV at 1.5 bar pressure, 0.10 mV at 1.25 bar pressure.
2) Feasibility of microchannels for slug channels was studied.
3) The difference in the output of experiment and simulation is because of the slug velocity being lower than that of the simulation for the same pressure.
4) Another reason for lower induced voltage of the experiments is the distortion of the slug. Slug distortion results in lower volume of ferrofluid entering and leaving the solenoid which means lower number of dipoles entering and leaving the solenoid.
5) The parametric study showed that increase in pressure and magnetization results in increase in the induced voltage.
6) Increase in the diameter shows increase the velocity of the slug and thus increase in the output voltage induced. However, for a given pressure the velocity keeps on increasing with the diameter until a certain limit. For example, 2.5 mm diameter is the limiting diameter for 2 bar pressure. Beyond this diameter the velocity of the slug starts to decrease.
7) The slug formation phenomenon is governed by the surface tension. As the diameter increases the surface tension starts getting weaker and the gravity effect takes its place. This results in decrease in slug velocity and failure to form the slug.
8) The length of the slug compared to coil is an important factor for voltage generation and thus accurate dispensing of ferrofluid volume is critical.

CHAPTER 7: FUTURE SCOPE

To determine the practical application of the energy harvesting principle, we looked at a paper discussing horizontal axis low wind energy harvesting device [20]. The paper explains that, the working of the low wind turbine is limited by two factors. Startup Wind Speed (U_s), which means minimum speed at which the turbines start rotating and Critical Wind Speed (U_c), which is the minimum speed at which the turbines attain the rpm to generate voltage. Thus, the voltage generation is limited even in the low wind turbines by the low wind velocity. We propose a device, which can generate the voltage by operating at these low wind speeds. The relationship between the windspeeds and shaft rotation speed is given by the following Fig 7-1 [20].

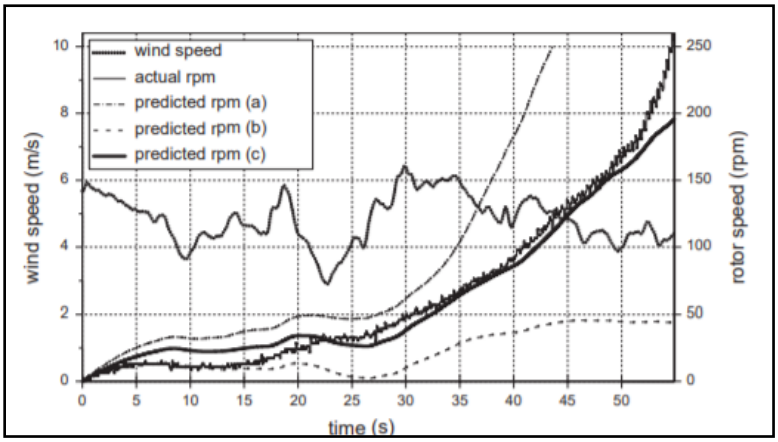

Fig 7-1 relation between the Windspeed and RPM of Turbine Blades [20]

We propose a device in which we trap a ferrofluid slug in air environment in capillary tube. The ends of capillary tube are connected to another capillary tube with U-tubes. This design facilitates the motion of the slug from end to end of the capillary tube while, the air pressure prevents it from escaping the tube. Also, the additional capillary leg helps to have mass conservation and facilitates the air flow. The design and schematic working of the design can be explained with the help of following Fig 7-2.

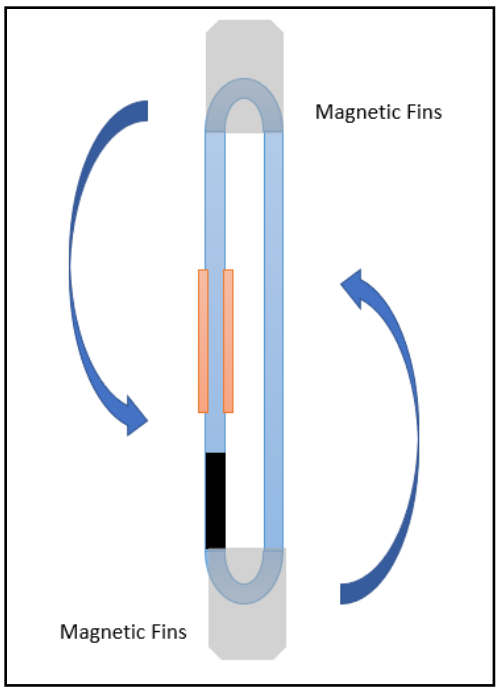

Fig 7-2 Proposed Design I of Energy Harvester

The one complete rotation of the device shown above, oscillates the slug in an out of the solenoid twice. That means for a rotation speed of 50 rpm, the frequency of slug oscillation that can be achieved is about 2.16 Hz. We propose this device to harvest the low wind energy by rotating it about its own axis.

Advantages of using Ferrofluid over permanent magnets:

- Ferrofluids being in liquid state can conform to any shape. This gives us the freedom of designing the device in any shape without any constraints.
- The wide flexibility of the design and liquid ferrofluid opens the possibilities of harvesting numerous types of ambient waste energy.
- Permanent magnets being in solid state will complicate the fabrication process. Also, using small cylindrical bar magnets instead of the slugs will give little control over the motion of the magnet.
- Adding the small solid permanent magnets will also increase the weight of the device and thus decrease the rotation it achieves for a given wind speed.

Disadvantages of using ferrofluids:

- Since ferrofluids are superparamagnetic in nature; presence of permanent magnetic field is always required to keep them magnetized.

As seen in the above discussion, the profits of using ferrofluids is far more than using permanent magnets. Thus, we can conclude that using ferrofluids for energy harvesting devices is more efficient option than permanent magnets.

REFERENCES

[1] https://en.wikipedia.org/wiki/Energy_harvesting

[2] https://en.wikipedia.org/wiki/Crystal_radio

[3] A. Kingatua," The How and Why of Energy Harvesting for Low-Power Applications", AllAboutCircuits.com 2016

[4] A. Bibo," Electromagnetic Ferrofluid based Energy Harvester", IEEE 2015.

[5] Jung," Feasibility Study on a New Energy Harvesting Electromagnetic Device Using Aerodynamic Instability, IEEE 2009

[6] Y. Wang," Ferrofluid Liquid Spring for Vibration Energy Harvesting", IEEE 2015.

[7] T. Reissman," Micro-solenoid Electromagnetic Power Harvesting for Vibrating Systems", SPIE 2008.

[8] A. Zimmerman Jones, "Electromagnetic Induction", Thought Co Blog 2018.

[9] Faraday's Law - https://en.wikipedia.org/wiki/Faraday%27s_law_of_induction

[10] Faraday's Law Image - https://www.electrical4u.net/electrical-basic/faradays-law-electromagnetic-induction/

[11] Faraday's Law Equations- http://hyperphysics.phy-astr.gsu.edu/hbase/electric/farlaw.html

[12] Lenz's Law - http://hyperphysics.phy-astr.gsu.edu/hbase/electric/farlaw.html

[13] Lenz's Law Image- http://hyperphysics.phy-astr.gsu.edu/hbase/electric/farlaw.html

[14] https://en.wikipedia.org/wiki/Ferrofluid

[15] EMG 700 - https://ferrofluid.ferrotec.com/products/ferrofluid-emg/water/

[16] EMG 901- https://ferrofluid.ferrotec.com/products/ferrofluid-emg/oil/

[17] EFH 1 - https://ferrofluid.ferrotec.com/products/ferrofluid-educational-fluid/efh/

[18] A. Shetye, "Experimental and Numerical Study of Marangoni Convection in Sandwiched Droplet", May 2016, M.S, The University of Texas at Arlington, 2016.

[19] D. Logan and D. Logan, A first course in the finite element method. Pacific Grove, CA: Brooks/Cole, 2002.

[20] A. Wright, D. Wood," The starting and low wind speed behavior of small horizontal axis turbine", Journal of Wind Engineering and Industrial Aerodynamics, 2004.

BIOGRAPHICAL INFORMATION

Omkar Amar Pawar completed his undergraduate degree in Mechanical Engineering from University of Mumbai, India, in 2015. He pursued his passion for research by joining University of Texas at Arlington in 2017. He is currently a member of Integrated Micro-Nano Fluidics Lab at UTA. He is also a Roger D. Goolsby Research Endowment Fellowship Awardee for AY 2018-19. His research interest lies in field of energy harvesting, thermal management and sustainable energy.